Semiconductor Physics, Quantum Electronics & Optoelectronics, 2007. V. 10, N 4. P. 31-35.

PACS 71.20.-b, 71.18.+y

Features of main band parameters for crystalline modification of Cd_3As_2 without center of symmetry

G.P. Chuiko and O.V. Dvornik
Kherson National Technical University, Department of General and Applied Physics
24, Beryslavske Sh., Kherson 73008, Ukraine, e-mail: chuiko@public.kherson.ua

Abstract. The so-called loops of extremes exist for the modification of Cd_3As_2 without the center of symmetry. The maximal spin splitting of bands is observable along a direction normal to the main crystalline axis. The number of topological transitions is increased for the surfaces of equal energy in all valence bands. The energies of the extremes of bands and topological transitions are calculated within the generalized Kane's and Kildal-Bodnar's model for a modification without the center of symmetry. It was established from the indirect solutions of the dispersion equation $k(\varepsilon)$ that the functions of the density of states near to the bottom of the conduction band change differently for different spin subbands with variation in energy. A similar situation is observed for the effective masses which demonstrate a nonlinear dependence on energy with a minimum caused by the degeneration of energy bands.

Keywords: center of symmetry, topological transformations, loops of extremes, spin splitting, density of states.

Manuscript received 15.08.07; accepted for publication 19.12.07; published online 31.01.08.

1. Introduction

Cadmium arsenide (Cd_3As_2) is an analog of the known zero-gap materials such as HgTe or HgSe. Its optical gap is as well negative, but the symmetry is tetragonal [1-3]. The crystalline modification stable at normal terms and with the spatial group of symmetry $I4_1cd - C_{4v}^{12}$ not only is tetragonal, but also is deprived of the center of symmetry. Such a combination is unique and hereby is perspective for practical applications as well as for theoretical investigations. One of the first attempts to show the peculiarities of the band structure and the density of states of this material has been made yet in [1] and recently in [2] as for their reflections on the kinematics of carriers.

Nevertheless, the full set of the topological transformations of the surfaces of equal energy, the peculiarities of both the density of states and the effective mass of carriers within the model of [3] are still not described completely, especially if the symmetry center is disappeared. The basic purposes of this paper follow from this previous sentence.

2. Theory

The generalized indirect dispersion law describing the spectra of carriers of the semiconductors without center of symmetry [4] can be written in a spherical system of coordinates as follows:

$$k_{p,m}^2(\varepsilon,u)=\left(\frac{\lambda(\varepsilon,u)}{2}\pm\sqrt{\left(\frac{\lambda(\varepsilon,u)}{2}\right)^2-\mu(\varepsilon,u)}\right), \qquad (1)$$

where $k_{p,m}^2(\varepsilon,u)$ is the square of the wave vector which depends on the energy and is a harmonic function of a spherical angle $u = \cos(\theta)$, and θ is the angle between the direction of the wave vector and the polar axis k_z, along which the main crystalline axis is directed. Each of the subscripts, "p" or "m", in (1) corresponds to one of two possible signs on the right-hand side of this expression. Thereto:

$$\lambda(\varepsilon,u)=2\left[\frac{\gamma(\varepsilon)}{F(\varepsilon,u)}+2\left(\frac{f_3(\varepsilon)}{F(\varepsilon,u)}\right)^2\left(1-u^2\right)\right], \qquad (2)$$

$$\mu(\varepsilon,u)=\left(\frac{\gamma(\varepsilon)}{F(\varepsilon,u)}\right)^2, \tag{3}$$

$$F(\varepsilon,u)=f_1(\varepsilon)+(f_2(\varepsilon)-f_1(\varepsilon))u^2. \tag{4}$$

The polynomials γ, f_1, f_2, and f_3 are the functions of both the energy of carriers (ε) and the model parameters:

$$f_1(\varepsilon)=P^2(\varepsilon+\delta+\Delta/3)(\varepsilon+\Delta/3)-\eta^{-2}P^2\Delta^2/9, \tag{5}$$

$$f_2(\varepsilon)=\eta^{-4}P^2\varepsilon(\varepsilon+2\Delta/3), \tag{6}$$

$$f_3(\varepsilon)=(1/3)\eta^{-1}P\Delta\xi\varepsilon, \tag{7}$$

$$\gamma(\varepsilon)=\varepsilon\Big((\varepsilon-\varepsilon_g)\big((\varepsilon+2\Delta/3)(\varepsilon+\delta+\Delta/3)-2\eta^{-2}\Delta^2/9\big)- -\xi^2(\varepsilon+2\Delta/3)\Big), \tag{8}$$

where ε_g, P, Δ are three known Kane's parameters [5]: ε_g is the optical gap; P is the matrix element of the quasipulse operator; Δ is the parameter of spin-orbit interaction; ξ and δ are two non-zero matrix elements of the crystalline potential, the first of them (ξ) takes the absence of a symmetry center into account [2-4], whereas the second is the parameter introduced in [6]; and $\eta=\frac{c}{2a}$ is the scaling parameter of a tetragonal deformation of the lattice [7].

If we take into account Eqs. (2)–(4) and Eqs. (5)–(8) for polynomials, two different and positive (what is a requisite within the spherical system) solutions for the moduli of the wave vectors will have the following form:

$$k_p(\varepsilon,u)\frac{1}{|F(\varepsilon,u)|}\times \times\sqrt{\gamma(\varepsilon)F(\varepsilon,u)+2f_3^2(\varepsilon)(1-u^2)+ +2|f_3(\varepsilon)|\sqrt{(1-u^2)(\gamma(\varepsilon)F(\varepsilon,u)+f_3^2(\varepsilon)(1-u^2))}}, \tag{9}$$

$$k_m(\varepsilon,u)=\frac{1}{|F(\varepsilon,u)|}\times \times\sqrt{\gamma(\varepsilon)F(\varepsilon,u)+2f_3^2(\varepsilon)(1-u^2)- -2|f_3(\varepsilon)|\sqrt{(1-u^2)(\gamma(\varepsilon)F(\varepsilon,u)+f_3^2(\varepsilon)(1-u^2))}}. \tag{10}$$

The digital values of parameters used in our computations are presented in Table 1.

Table 1.

ε_g, eV	P, eV·m	Δ, eV	δ, eV	ξ, eV	η	a, Å	c, Å
–0.13	$7.0\times\times10^{-10}$	0.27	0.095	0.035	1.004726	12.6461	25.4908

3. Results of computations and their discussion

The dispersion law in Cd_3As_2 is anisotropic. This is seen both from Eqs. (1)-(4) and Fig. 1, where the edges of bands have obvious curvatures. The only exception is the bottom of the conduction band, just this energy is absolutely independent of the direction (thus, of θ). Such a kind of anisotropy of energies of the band edges is observable if the parameter $\delta\neq0$, i.e. also for the modifications with the symmetry center: $\xi=0$. However, the width of the band of light holes and especially that of the band of heavy holes are noticeably different for the carriers in the opposite spin states under condition $\xi\neq0$, i.e. for the modification without the symmetry center. Moreover, the absence of the symmetry center leads to the splitting of the band states into two spin subbands, because the Kramer's degeneration was over. It is explicitly shown in Fig. 2. It is also seen from Eqs. (9) and (10), that both different solutions describe the splitting of subbands into the space of wave vectors.

Consequently, it is even possible to indicate some intervals of energies (true, that they are rather narrow) and directions, inside which just the carriers with one from the two possible spin states can exist. Such a "separation effect" is especially valid for the bottom of the band of light holes and for the top of the band of heavy carriers in a close proximity of the direction $\theta\to\frac{\pi}{2}$, i.e. normally to the main crystalline

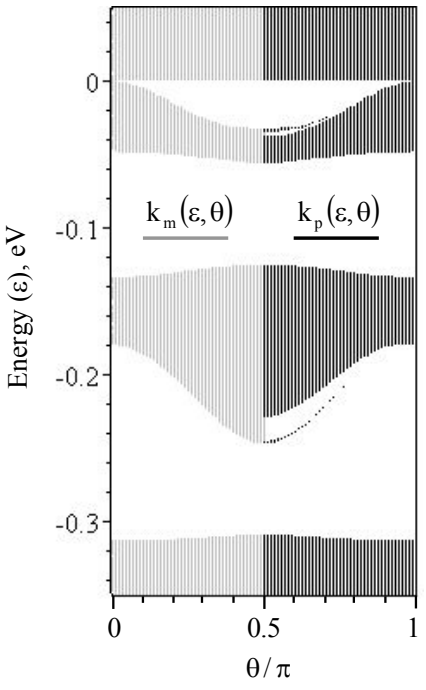

Fig. 1. Diagram of the distribution of allowed (they are shaded) and forbidden states for four actual energy bands of Cd_3As_2.

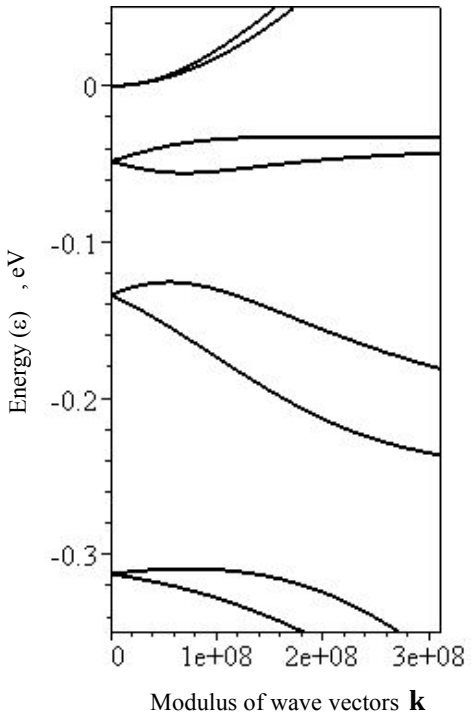

Fig. 2. Energy band structure of Cd_3As_2 for $u = 0$ ($\theta = \pi/2$). The zero of energy coincides with the bottom of the conduction band.

axis. The maximal width of the band of heavy holes in Cd_3As_2 without center of symmetry is observed in the direction θ = 0, i.e. along the main crystalline axis. Opposite, the maximal width of the band of light holes is observed in the direction $\theta = \frac{\pi}{2}$. The extremes of the bands (except only for the conduction band) are displaced from the Γ point ($\mathbf{k} = \mathbf{0}$). A similar situation, i.e. the appearance of the so-called "loops of extremes", is observed not only in this material, but in many materials with the single main crystalline axis.

The condition

$$\left|F(\varepsilon,u)\right| = 0 \qquad (11)$$

allows us to define the points of divergence of solutions (9) and (10). The positive solutions of the above equation for the functions $u(\varepsilon)$ would characterize the singular directions with additional limitations imposed by the nature of the function $u^2(\varepsilon) = \cos(\theta)^2$:

$$u_1(\varepsilon) = \sqrt{\frac{f_1(\varepsilon)}{f_1(\varepsilon) - f_2(\varepsilon)}}; \quad 0 \le u_1^2(\varepsilon) \le 1. \qquad (12)$$

Just the positive values of the square root are worth to be accounted because the parameter u is included everywhere only as u^2. Solving Eqs. (12) with the boundary conditions $u_1(\varepsilon) = 0$ and $u_1(\varepsilon) = 1$ for the energy allow us to get the characteristic energies of topological transformations in the bands and/or some extremes of them. These above-mentioned solutions can be got properly as four roots of the polynomials $f_1(\varepsilon)$ and $f_2(\varepsilon)$. Moreover, these peculiarities would be discernible both for modifications with the center of symmetry and for the modification without it in view of the fact that Eqs. (11) and (12) contain neither the function $f_3(\varepsilon)$ on the whole nor its factor ξ as a parameter.

The condition of reality of solutions (9) and (10) requires that the radicands be nonnegative. This means that positive solutions of the equation:

$$\left(\gamma(\varepsilon)F(\varepsilon,u) + f_3^2(\varepsilon)\left(1-u^2\right)\right) = 0 \qquad (13)$$

for the function $u(\varepsilon)$ would characterize the further singular directions with the same limitations imposed by nature of the function $u^2(\varepsilon) = \cos(\theta)^2$:

$$u_2(\varepsilon) = \sqrt{\frac{\gamma(\varepsilon)f_1(\varepsilon) + f_3^2(\varepsilon)}{\gamma(\varepsilon)f_1(\varepsilon) + f_3^2(\varepsilon) - \gamma(\varepsilon)f_2(\varepsilon)}};$$

$$0 \le u_2^2(\varepsilon) \le 1. \qquad (14)$$

Note that Eq. (14) transforms to Eq. (12), if $f_3(\varepsilon) \to 0$. This indicates that the modifications without the symmetry center might have more singularities. Indeed, by solving the equations $u_2(\varepsilon) = 0$ and $u_2(\varepsilon) = 1$, we can get the extreme points and/or the points of extra topological transformations for the modification without the symmetry center. Obviously, this system of solutions is more rich in content, than the collection of four roots of polynomials $f_1(\varepsilon)$ and $f_2(\varepsilon)$ mentioned above.

The common picture of the behavior of the functions $u_1(\varepsilon)$ and $u_2(\varepsilon)$ is given in Fig. 3. We mark also all specific points on the energy scale. Table 2 gives a more detailed list of them and contains information about the sequence of transformations as for the surfaces of equal energy. The lines in Fig. 3 show the boundaries between allowed and forbidden states and thus are associated openly with Fig. 1. Such an understanding allows us to easily classify each of the specific points of Fig. 3 what has been reflected inside Table 2. We point out only that the disappearance of the symmetry center causes the arising of four extra topological transformations: two for heavy holes band and two inside each of the other valence bands.

The general expressions for the functions of the density of states and for the corresponding effective masses can be written down as follows:

$$g_{p,m}(\varepsilon) = \frac{\partial N_{p,m}(\varepsilon)}{\partial \varepsilon} = \frac{1}{6\pi^2}\left(\frac{\partial}{\partial \varepsilon}\left(\int_a^b k_{p,m}^3(\varepsilon,u)du\right)\right), \qquad (15)$$

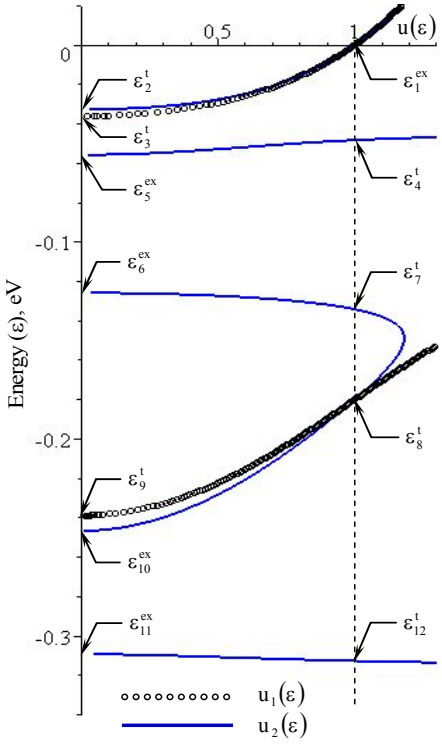

Fig. 3. Dependences of $u_1(\varepsilon)$, $u_2(\varepsilon)$ and the set of singular points.

$$m_{p,m}(\varepsilon)=\left(\frac{\pi^2\hbar^2}{m_0 e}\right)\left(\frac{1}{3\pi^2 N_{p,m}(\varepsilon)}\right)^{\frac{1}{3}} g_{p,m}(\varepsilon). \qquad (16)$$

Here, the functions $k_{p,m}(\varepsilon,u)$ are given by Eqs. (9) and (10), and $[a,b]$ is the integration interval which provides the reality and the integrity of these functions. The constants m_0, e are the mass and the elementary charge of a free electron, respectively. Expressions (15) and (16) look to be simple. However, "devil likes to be hidden in details". Such a detail supposed the accurate determination of the integration intervals $[a,b]$ on the each of the energy intervals shown in Table 2 and Fig. 3. This problem was solved using the data of Figs. 1 and 3 and Table 2. The results are presented in Table 3.

We give here merely the results of computations for the conduction band, because all experimental data were obtained up to now just for the samples of the *n*-type. The extremely narrow width of two bands of holes (see Fig. 1), which are divided into a few thinner intervals of the integration by the topological transformations, make the corresponding computations nothing more than academic exercises. Such results cannot be trustworthy from the physical point of view and, what's more, they have no possibilities for a comparison with experimental data.

Table 2.

Singular points	Energies, eV	Conditions	Description	Type of surface of equal energy or type of topological transition	Notes
ε_1^{ex}	0	$u_1(\varepsilon)=1$; $u_2(\varepsilon)=1$	Bottom of the conduction band and the top of the band of heavy holes	ETC, H2	Bands are degenerated just under present conditions
ε_2^t	–0.03263	$u_2(\varepsilon)=0$	Extra topological transformation	H2 → H1	Only for the modification without the symmetry center
ε_3^t	–0.03611	$u_1(\varepsilon)=0$	Topological transformation	H1 → ETC	
ε_4^t	–0.04823	$u_2(\varepsilon)=1$	Extra topological transformation	ETC → ET	Only for the modification without the symmetry center
ε_5^{ex}	–0.05573	$u_2(\varepsilon)=0$	Bottom of the band of heavy holes	ET	
ε_6^{ex}	–0.12577	$u_2(\varepsilon)=0$	Top of the band of light holes	ET	For the modification with the symmetry center ε_6^{ex} = –0.13000 eV
ε_7^t	–0.13410	$u_2(\varepsilon)=1$	Extra topological transformation	ET → ETC	Only for the modification without the symmetry center
ε_8^t	–0.18000	$u_1(\varepsilon)=1$; $u_2(\varepsilon)=1$	Topological transformation	ETC → H1	
ε_9^t	–0.23889	$u_1(\varepsilon)=0$	Topological transformation	H1 → ET	
ε_{10}^{ex}	–0.24663	$u_2(\varepsilon)=0$	Bottom of the band of light holes	ET	
ε_{11}^{ex}	–0.30924	$u_2(\varepsilon)=0$	Top of the spin splitting band	ET	
ε_{12}^t	–0.31267	$u_2(\varepsilon)=1$	Extra topological transformation	ET → ETC	Only for the modification without the symmetry center

Notations:
- H1, H2 – Hyperboloid with one or two cavity, respectively;
- ET, ETC – Elliptic toroid or elliptic toroid with self-crossing, respectively.

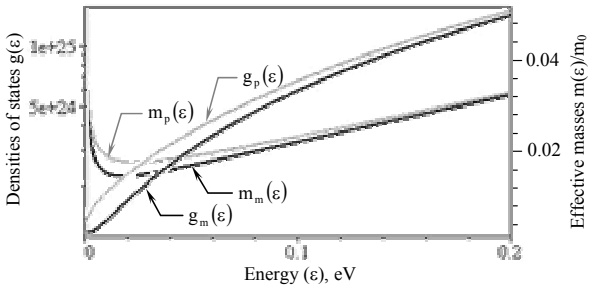

Fig. 4. Dependences of $g(\varepsilon)$ and $m(\varepsilon)$ for both subbands of the conduction band of Cd_3As_2.

Table 3.

$[a, b]$	$[0,1]$	$[0,u_2(\varepsilon)]$	$[u_2(\varepsilon),u_1(\varepsilon)]$	$[0,u_1(\varepsilon)]$	$[u_1(\varepsilon),1]$
Energy intervals	$[\varepsilon_1^{ex},\infty]$	$[\varepsilon_5^{ex},\varepsilon_4^t]$			
	$[\varepsilon_4^t,\varepsilon_3^t]$	$[\varepsilon_7^t,\varepsilon_6^{ex}]$	$[\varepsilon_2^t,\varepsilon_1^{ex}]$	$[\varepsilon_9^t,\varepsilon_8^t]$	$[\varepsilon_3^t,\varepsilon_1^{ex}]$
	$[\varepsilon_8^t,\varepsilon_7^t]$	$[\varepsilon_9^t,\varepsilon_{10}^{ex}]$	$[\varepsilon_9^t,\varepsilon_8^t]$		
	$[-\infty,\varepsilon_{12}^t]$	$[\varepsilon_{11}^{ex},\varepsilon_{12}^t]$			

Figure 4 presents the densities of states and the effective masses of electrons as functions of the energy. We can see that the spin splitting decreases gradually with increase in the energy. The nonlinear part of the dependence of effective masses on the energy with one apparent minimum is situated in the low-energy range.

4. Conclusions

1. The disappearance of the symmetry center at the phase transition $P4_2/nbc \rightarrow I4_1cd$ ($D_{4h}^{11} \rightarrow C_{4v}^{12}$) causes the arising of four additional transformations of the topology of the surfaces of equal energy inside each of the hole bands.
2. The disappearance of the symmetry center leads to the spin breaking up not only for the energy bands, but also for the densities of the states in them and the effective masses of carriers.
3. The palpable nonlinearities of the dependences of effective masses on the energy, as well as the existence of their minima near the bottom of the conduction band, are evidently forced by the actual degeneration of the conduction band with the band of heavy holes.

Acknowledgements

The authors thank Dr. Stanislaw Shutov for his helpful participation in the preparation of this paper and for many fruitful discussions.

References

1. G.P. Chuiko, I.A. Teplinskaya, The topological transition and a relevant singularity in the density of states of the conduction band as characteristic properties of inversive tetragonal semiconductor – cadmium arsenide // *Fizika Tekhnika Poluprovodnikov* **17**(6), p. 1123-1125 (1983) (in Russian).
2. G. Chuiko, N. Don, V. Martyniuk and D. Stepanchikov, Effect of symmetry center losses on energy bands and carrier kinematics in Zn_3As_2 and Cd_3As_2 // *Semiconductor Physics, Quantum Electronics & Optoelectronics* **9**(2), p. 17-22 (2006).
3. G. Chuiko, O. Dvornik, and V. Ivchenko, Generalized Kildal-Bodnar's dispersion law for 4mm (C_{4V}) ordering crystals // *Ukr. Fizych. Zhurnal* **45**(10), p. 1188-1192 (2000) (in Ukrainian).
4. G.P. Chuiko, O.V. Dvornik, D.M.Stepanchikov, Peculiarities of the dispersion law in crystals of class $\mathbf{A_3^{II}B_2^V}$ // *Vestnik Kherson. Gosudarstv. Tekhnichesk. Universiteta* **3**(16), p. 32-37 (2002) (in Russian).
5. E.O. Kane, Band structure of indium antimonide // *J. Phys. Chem. Solids* **1**, p. 249-261 (1957).
6. H. Kildal, Band structure of $CdGeAs_2$ near k=0 // *Phys. Rev. B* **10**(12), p. 5082-5087 (1974).
7. A.M. Polubotko, Dependence of parameters of the Kildal-Bodnar's dispersion law on the value of tetragonal compression in chalcopyrites // *Fizika Tekhnika Poluprovodnikov* **19**(4), p. 772-774 (1983) (in Russian).